The role of curvature in the slowing down acceleration scenario

Víctor H. Cárdenas* and Marco Rivera†
Departamento de Física y Astronomía, Facultad de Ciencias, Universidad de Valparaíso, Gran Bretaña 1111, Valparaíso, Chile

We introduce the curvature Ω_k as a new free parameter in the Bayesian analysis using SNIa, BAO and CMB data, in a model with variable equation of state parameter $w(z)$. We compare the results using both the Constitution and Union 2 data sets, and also study possible low redshift transitions in the deceleration parameter $q(z)$. We found that, incorporating Ω_k in the analysis, it is possible to make all the three observational probes consistent using both SNIa data sets. Our results support dark energy evolution at small redshift, and show that the tension between small and large redshift probes is ameliorated. However, although the tension decreases, it is still not possible to find a consensus set of parameters that fit all the three data set using the Chevalier-Polarski-Linder CPL parametrization.

PACS numbers: 98.80.Cq

I. INTRODUCTION

Since 1998 one of the biggest puzzles in cosmology is dark energy: the unknown component responsible for the current accelerated expansion of the universe [1]. In its simpler form, this can be described by a constant equation of state parameter $w = -1$, corresponding to a cosmological constant, leading to the ΛCDM model, the simplest model that fits a varied set of observational data.

As the observations increase in precision, it is possible to reach levels that enable us to discriminate between a cosmological constant or a dynamical cosmological constant ($w = w(z)$). The source of this dynamical dark energy could be both, a new field component filling the universe, as a quintessence scalar field [2], or it can be produced by modifying gravity [3].

In a recent paper [4] the authors suggest that current observational data could favor a scenario in which the acceleration of the expansion has past a maximum value and is now decelerating. The key point in deriving this conclusion is the use of the Chevalier-Polarski-Linder (CPL) parametrization [5], [6] for a dynamical equation of state parameter

$$w(a) = w_0 + (1 - a)w_1, \tag{1}$$

where w_0 and w_1 are constants to be fixed by observations and a is the scale factor. An updated analysis performed using recent SNIa data was informed in [7] where similar conclusions were derived. Both analysis assumed a flat universe.

Although it is often said that the inflationary scenario predicts a flat universe [9], the situation has not been settled down yet, in part because the observations are not conclusive and because in theory $\Omega_k = 0$ is not the only solution [10]. In fact, the conclusion deduced from the analysis of the observations using a w =constant, implying a model with cosmological constant $|1 + w| < 0.06$, only works if we assumed a flat universe. However, considering the curvature as a new free parameter, it leads to an increment in the uncertainties in all the others parameters. In particular, in the context of models with dynamical dark energy, a number of works have discussed the degeneracies between $w(z)$ and Ω_k [11] [12] [13] [14] [15].

It is the purpose of this paper to enhance the analysis of this phenomenon, relaxing the assumption of a flat universe, considering explicitly the geometric degeneracy between Ω_k and $w(z)$. This enable us to explore new features considering the CPL parametrization, enabling us to accommodate a similar behavior for $q(z)$ using all the three observational test. This fact again shows the sensitivity of the observational data to even smaller values of the curvature parameter. The result found here shows that a single trend for $q(z)$ is possible to draw using all the three observational probes, ameliorating the tension between data sets.

The paper is organized as follows: in the next section we re-study the flat universe case using both SNIa data sets [16], [17]. Then, we show how to generalize the analysis considering a curved universe, in section III, which are our main results. We end that section with a discussion.

II. A FLAT UNIVERSE ANALYSIS: UNION2 VERSUS CONSTITUTION DATA

The original analysis [4] was performed using the Consitution data set [16] of SNIa. In this section we reanalyze this data set along the BAO and CMB constraints using the CPL parametrization. Then, we repeat the analysis using the full Union2 data sample [17], looking for differences in the consequences derived from these analysis. We end this section discussing our results along the ones obtained in the recent work [7].

*Electronic address: victor[at]dfa.uv.cl
†Electronic address: marco.rivera[at]uv.cl

The luminosity distance in a flat universe is

$$d_L(z) = (1+z)\frac{c}{H_0}\int_0^z \frac{dz'}{E(z')}, \quad (2)$$

where

$$E^2(z) = \Omega_m(1+z)^3 + (1-\Omega_m)e^{3\int_0^z \frac{1+w(z')}{1+z'}dz'}. \quad (3)$$

The SNIa data give the distance modulus $\mu_{obs}(z)$ as a function of redshift. We fit the SNIa with the cosmological model by minimizing the χ^2 value defined by

$$\chi^2_{SNIa} = \sum_{i=1}^{Np} \frac{[\mu(z_i) - \mu_{obs}(z_i)]^2}{\sigma^2_{\mu i}}, \quad (4)$$

where $\mu(z) \equiv 5\log_{10}[d_L(z)/Mpc] + 25$ is the theoretical value of the distance modulus, and Np is the number of data points.

The BAO data considered in our analysis is the distance ratio obtained at $z = 0.20$ and $z = 0.35$ from the joint analysis of the 2dF Galaxy Redsihft Survey and SDSS data [18], that can be expressed as

$$\frac{D_V(0.35)}{D_V(0.20)} = 1.736 \pm 0.065, \quad (5)$$

with

$$D_V(z_{BAO}) = \left[\frac{z_{BAO}}{H(z_{BAO})}\left(\int_0^{z_{BAO}} \frac{dz}{H(z)}\right)^2\right]^{1/3}. \quad (6)$$

We fit the cosmological model minimizing the χ^2 defined by

$$\chi^2_{BAO} = \frac{[D_V(0.35)/D_V(0.20) - 1.736]^2}{0.065^2}. \quad (7)$$

A result from the combination of SNIa and BAO is given by a joint analysis finding the best fit parameters that minimize $\chi^2_{SNIa} + \chi^2_{BAO}$.

In addition, we incorporate to the analysis the CMB shift parameter [19], which is the reduce distance at $z_{ls} = 1090$ [20]

$$R = \sqrt{\Omega_m H_0^2} r(z_{ls}) = 1.71 \pm 0.019. \quad (8)$$

Here we use the comoving distance $r(z)$ from the observer to redshift z which is related to the luminosity distance by $d_L(z) = (1+z)r(z)$. In this case we compute χ^2 by

$$\chi^2_{CMB} = \frac{[R - 1.71]^2}{0.019^2}, \quad (9)$$

to find out the result from CMB and the constraints from SNIa+BAO+CMB are given by $\chi^2_{SNIa} + \chi^2_{BAO} + \chi^2_{CMB}$.

For the CPL parametrization, $w = w_0 + w_1 z/(1+z)$, the second term in the righ hand side of (3) is

$$(1-\Omega_m)(1+z)^{3(1+w_0+w_1)}\exp\left(-\frac{3w_1 z}{1+z}\right). \quad (10)$$

TABLE I: The best fit values for the free parameters using the Constitution data set in the case of a flat universe model. See the related Fig. 1.

Data Set	χ^2_{min}	Ω_m	w_0	w_1
SN	461.23	0.4519	-0.2209	-11.228
SN+BAO	461.60	0.4551	-0.1253	-12.255
SN+BAO+CMB	466.94	0.2578	-0.9275	-0.019

Using the Constitution sample consisting of 397 data points, assuming a flat universe, leads to the results shown in Table I. They are very similar to the ones informed in [4] and [8]. Given the number of degrees of freedom N, a good estimate of the width of the χ^2 distribution is $\sigma = \sqrt{2/N}$, which in our case gives $\sigma \simeq 0.07$, a number taken into account to discriminate statistical significance among different runs. Having found these numbers, we can draw a profile of the deceleration parameter $q = -\ddot{a}a/\dot{a}^2$ as a function of the redshift z for each case. This is shown in Fig.1. Clearly, the incorporation of the CMB constraints into the fitting process, leads to a completely different behavior for $q(z)$. The values of χ^2_{min} show that the CPL parametrization is unable to fit the data simultaneously at low and large redshift. Because the best fit considering CMB gives a

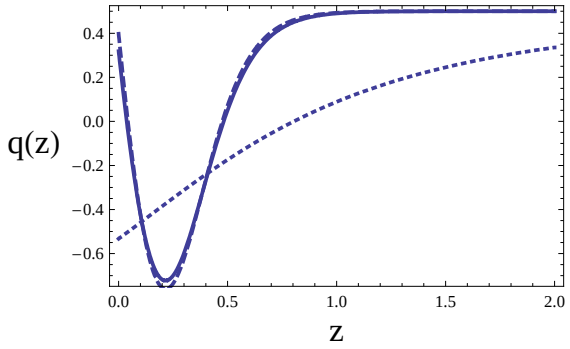

FIG. 1: Using the Constitution data set [16] we plot the deceleration parameter reconstructed using the best fit values for three cases: only SNIa (continuous line), SNIa+BAO (dashed line) and SNIa+BAO+CMB (dotted line).

χ^2_{min} 5 points higher than those considering SNIa and SNIa+BAO, indicates that CMB data favor a different behavior at small redshift, as the one observed in Fig.1. Considering the reduced χ^2 we notice that $\chi^2_{red} = 1.169$ for SNIa+BAO and $\chi^2_{red} = 1.182$ for SNIa+BAO+CMB, showing that using SNIa+BAO gives a much better fit to the model than the one using CMB, and again the inadequacy of the CPL parametrization of fitting data at large and small redshift. The same can be concluded observing Figure 2 where the confidence contours in the $w_0 - w_1$ plane is plotted . Notice that the ellipses corresponding to SNIa alone and SNIa+BAO are almost identical, but the one considering CMB data does not overlap the others, indicating the tension between these data sets.

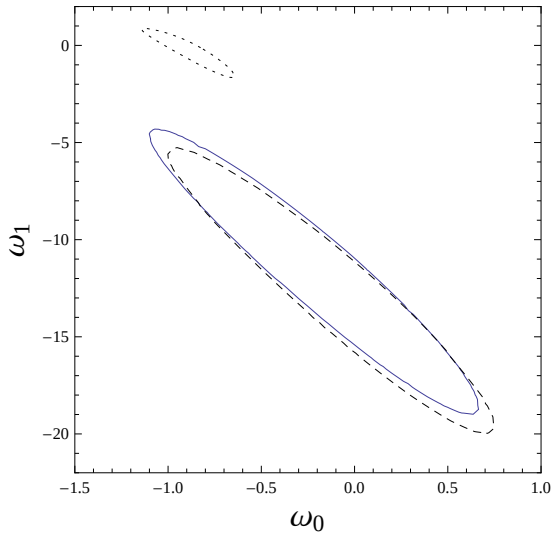

FIG. 2: Using the Constitution data set [16] we plot the 1σ contours for the $w_0 - w_1$ parameters using the best fit values for three cases: only SNIa (continuous line), SNIa+BAO (dashed line) and SNIa+BAO+CMB (dotted line).

Using the Union 2 set [17], the largest SNIa luminosity distance sample currently available, consisting in 557 type Ia supernovae, the analysis leads to the results shown in Table II. In this case, $\sigma \simeq 0.06$, then again

TABLE II: The best fit values for the free parameters using the Union 2 data set in the case of a flat universe model. See also Fig. 3.

Data Set	χ^2_{min}	Ω_m	w_0	w_1
SN	541.43	0.4197	-0.8632	-5.490
SN+BAO	542.11	0.4281	-0.7959	-6.537
SN+BAO+CMB	543.91	0.2547	-0.9979	0.190

the numbers quoted in the table have a trustable statistical meaning. However, by comparing this with the results using the Constitution data set, we observe that the difference between the case with and without the CMB data is now smaller ($\simeq 1.8$), although still large compared to $3\sigma = 0.18$. Plotting the deceleration parameter using these numbers leads to Fig.3. Again, the case SNIa alone and SNIa+BAO are almost identical, but the case including CMB data does not shown the rapid change at small redshift as is also found using the Constitution data set. Similar results were recently published in [7]. Meanwhile the statistical analysis using the Constitution data set give χ^2_{red} values greater than one, indicating bad fittings, the ones obtained using the Union 2 sample, gives us over-fitting values, $\chi^2_{red} < 1$. This is important to notice, because an over-fitting work indicates that probably we are fitting noise instead of the actual relationship, and then more data would be necessary to improve the predictive power of the model. Therefore, it is necessary to perform a study that compares both data sets of SNIa to

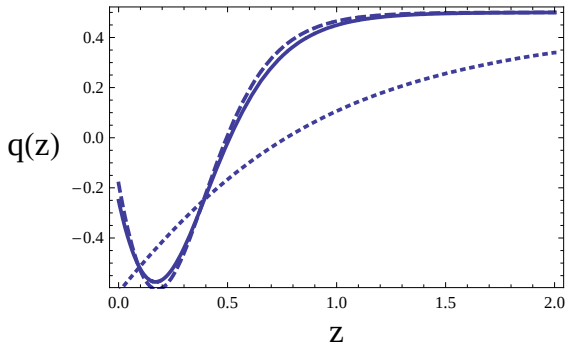

FIG. 3: Using the Union 2 data set [17] we plot the deceleration parameter reconstructed using the best fit values for three cases: only SNIa (continuous line), SNIa+BAO (dashed line) and SNIa+BAO+CMB (dotted line).

shed some light on this point.

This fact can also be viewed from Figure 4 where confidence contours in the $w_0 - w_1$ plane are plotted. Notice that again, the ellipses corresponding to SNIa alone and SNIa+BAO are similar, but the one considering SNIa+BAO+CMB points into a completely different region. This confirm the previous claim that the CPL parametrization is not adequate here.

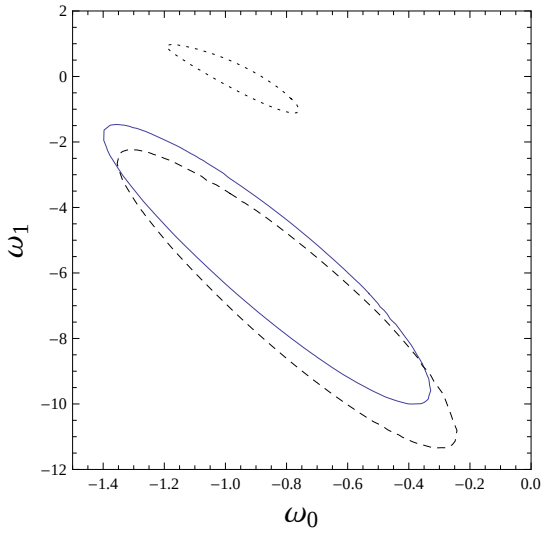

FIG. 4: Using the Union 2 data set [17] we plot the 1σ contours for the $w_0 - w_1$ parameters using the best fit values for the three cases: only SNIa (continuous line), SNIa+BAO (dashed line) and SNIa+BAO+CMB (dotted line).

TABLE III: The best fit values for the free parameters using the Constitution data set in the case of a non flat universe model. See Fig. 5.

Data Set	χ^2_{min}	Ω_m	w_0	w_1	Ω_k
SN	459.15	0.7049	-0.4698	-3.6307	-0.9901
SN+BAO	459.37	0.6861	-0.4868	-2.8019	-1.1534
SN+BAO+CMB	461.14	0.4934	-0.1625	-11.2574	-0.0886

III. RELAXING THE FLAT UNIVERSE ASSUMPTION

The comoving distance from the observer to redshift z is given by

$$r(z) = \frac{c}{H_0}\frac{1}{\sqrt{-\Omega_k}}\sin(\sqrt{-\Omega_k}\Gamma(z)) \quad (11)$$
$$\Gamma(z) = \int_0^z \frac{dz'}{E(z')},$$

where $\Omega_k = -k/H_0^2$, k being the curvature constant and

$$E^2(z) = \Omega_m(1+z)^3 + \Omega_k(1+z)^2 + \Omega_{de}f(z), \quad (12)$$
$$f(z) = \exp\left\{3\int_0^z \frac{1+w(z')}{1+z'}dz'\right\},$$

and $\Omega_{de} = 1 - \Omega_m - \Omega_k$.

For the CPL parametrization, $w = w_0 + w_1 z/(1+z)$, the function $f(z)$ in (12) leads to

$$f(z) = (1+z)^{3(1+w_0+w_1)}\exp\left(-\frac{3w_1 z}{1+z}\right). \quad (13)$$

Using the Constitution set we found the results displayed in table III. A direct comparison with the result of table I, where $\Omega_k = 0$ was assumed, shows many interesting changes. In general, all the values for χ^2_{min} are lower considering Ω_k a free parameter. This result is expected, but the best fit values obtained are not. For example, in the cases where SNIa and SNIa+BAO are considered, the best fit values are completely different: Ω_k is around -1, meanwhile the value for w_1 is four times less negative than in the flat case. Also the matter density becomes almost twice the value that in the flat case.

Using the best fit values of the parameters we plot $q(z)$ versus z for each case. We see from Fig.5, that all the three cases behaves in a similar way. This is one of the main result of our work: the joint analysis SNIa+BAO+CMB using the curvature shows qualitatively the same variation in $q(z)$ for small redshift than those for SNIa alone or SNIa+BAO, a results that as far as we know has not been informed previously.

The SNIa alone and SNIa+BAO look very similar to the already known, with the exception that $q(z)$ is almost reaching its zero value today $z = 0$. In each run, we have explored several different initial conditions, to find the best fit values. Regarding the case where is used SNIa+BAO+CMB, using a small value for $\Omega_k = -0.089$, enable us to find a $q(z)$ whose form follows the same trend that the previous cases. Here we must emphasize three important points: first, the present value of the deceleration parameter is positive today ($z = 0$), indicating that our universe is now decelerating, having crossed to positive values at $z \simeq 0.1$. Second, the form of $q(z)$ shows that even considering the CMB data, the incorporation of the curvature to the analysis allows a transition in the deceleration parameter at small redshift $z < 0.3$. And finally, although the SNIa+BAO+CMB case fit a $q(z)$ that change sign, the profile of $q(z)$ reaches a minimum value later (at $z \simeq 0.2$) than in the other two cases ($z \simeq 0.4$), crossing to negative values later than the other cases and also in the SNIa+BAO+CMB case the asymptotic value $q \simeq 1/2$ for $z > 1$ is less than the one found in the other cases $q \simeq 1$. However, this results does not imply that the tension between low and high redshift data has disappeared. In fact, by drawing confidence contours around the best fit values in the $w_0 - w_1$ plane shown in figure 8, again the ellipses at one sigma does not overlap at all, even those for SNIa and SNIa+BAO.

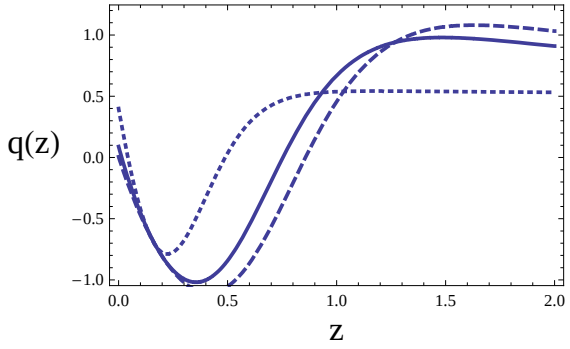

FIG. 5: Using the Constitution data set [16] we plot the deceleration parameter reconstructed using the best fit values for three cases: only SNIa (continuous line), SNIa+BAO (dashed line) and SNIa+BAO+CMB (dotted line).

TABLE IV: The best fit values for the free parameters using the Union 2 data set in the case of a non flat universe model. See Fig. 7.

Data Set	χ^2_{min}	Ω_m	w_0	w_1	Ω_k
SN	541.05	0.2973	-0.4362	-19.343	0.3551
SN+BAO	541.91	0.3433	-0.5488	-14.531	0.2499
SN+BAO+CMB	542.18	0.4449	-0.8180	-5.1670	-0.0744

Using the larger Union 2 data set [17] we performed the same analysis as before obtaining the best fit parameter shown in table IV. The cases corresponding to SNIa data only and the joint analysis of SNIa and BAO data, behaves similarly to the ones already displayed using the Constitution data set as is evident in Fig.7. However in this case the change in sign of $q(z)$ take place later than the ones discussed in Fig.5. Actually, this time

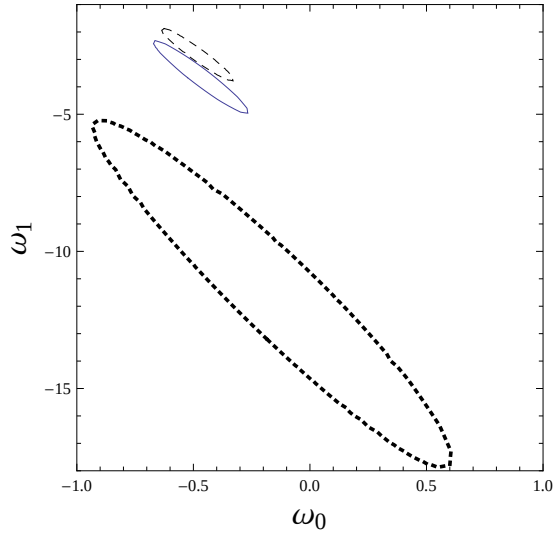

FIG. 6: Using the Constitution data set [16] we plot the 1σ contours for the $w_0 - w_1$ parameters using the best fit values for three cases: only SNIa (continuous line), SNIa+BAO (dashed line) and SNIa+BAO+CMB (dotted line).

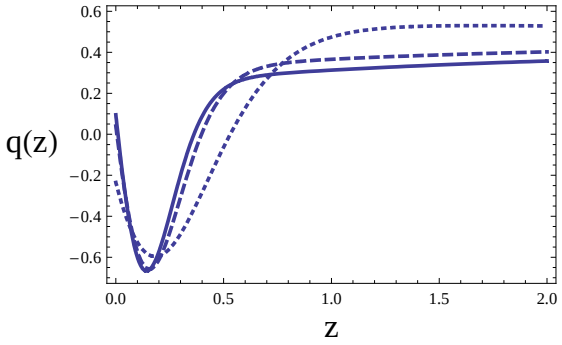

FIG. 7: Using the Union 2 data set [17] we plot the deceleration parameter reconstructed using the best fit values for three cases: only SNIa (continuos line), SNIa+BAO (dashed line) and SNIa+BAO+CMB (dotted line).

all the three fits behave similarly, reaching a minimum value at $z \simeq 0.2$. Again, the value of the deceleration parameter today is almost zero for the SNIa alone and SNIa+BAO cases, indicating that the acceleration of the expansion of the universe had already ceased, and in the SNIa+BAO+CMB case q is small but still negative. However, as was also the case using the Constitution set, the concordance in the profile of $q(z)$ among the observational probes is only apparent, because the one sigma confidence contours in the plane $w_0 - w_1$ indicate that although SNIa and SNIa+BAO share a region in that phase space, the CMB data spoiled the agreement.

Comparing table I with III, and II and IV, we observe that the incorporation of the curvature parameter decreases the value of χ^2_{min}, indicating that a model with a non flat universe is preferred, even with a small value. Also is clear from the analysis that, both in the flat and non flat case, using the Constitution data set, leads to a wrong fit $\chi^2_{red} > 1$, meanwhile using the Union 2 data set, leads to a over-fitting, $\chi^2_{red} < 1$, indicating the necessity of a further analysis of these SNIa data sets.

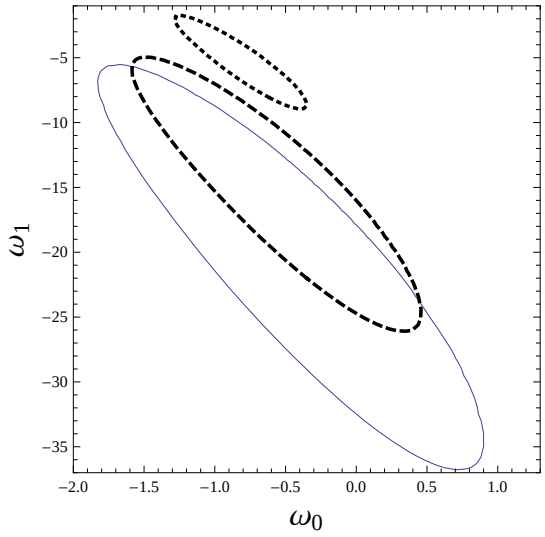

FIG. 8: Using the Union2 data set [17] we plot the 1σ contours for the $w_0 - w_1$ parameters using the best fit values for three cases: only SNIa (continuous line), SNIa+BAO (dashed line) and SNIa+BAO+CMB (dotted line).

One of the main result from this analysis is that, the incorporation of the curvature as a new free parameter, enable us to accommodate a similar behavior for $q(z)$ using all the three observational test. This fact again shows the sensitivity of the observational data to even smaller values (see Table IV) of the curvature parameter. The result found here shows that a single trend for $q(z)$ is possible to draw using all the three observational probes, ameliorating the tension between data sets.

In this paper we have shown that incorporating the curvature Ω_k as a free parameter in the Bayesian analysis using SNIa, BAO and CMB, enable us to ameliorate the tension between low and high redshift found in previous works [4],[7]. This is explicitly shown using both the Constitution [16] and the recent Union 2 [17] data sets. Even considering small values for the curvature parameter, it is possible to find a general behavior for $q(z)$ at small redshift which shows a rapid variation in sign between $z \simeq 0.5$ to $z \simeq 0$. Because the CPL ansatz (1) implicitly assumes that nothing special occurs for DE in the redshift interval between $z = 0$ to $z \simeq 2$, the trend found in this work shows the incompatibility of the CPL parametrization in describing the variation of $w(z)$ with redshift. This conclusion is reinforced based on the lack of overlap among the confidence contours in the three cases in the $w_0 - w_1$ plane.

Acknowledgments

The authors want to thanks Sergio del Campo for useful discussions. This work was supported by Grant DIUV N° 13/09 from Universidad de Valparaíso and FONDECYT Grant N° 1110230.

[1] M. Sami, arXiv: 0904.3445 [hep-th]; J. Frieman, M. Turner and D. Huterer, Ann. Rev. Astron. Astrophys. **46**, 385 (2008); T. Padmanabhan, Gen. Rel. Grav. **40**, 529 (2008); M.S. Turner and D. Huterer, J. Phys. Soc. Jap. **76**, 111015 (2007); N. Straumann, Mod. Phys. Lett. **A21** 1083 (2006); E.J. Copeland, M. Sami and S. Tsujikawa, Int. J. Mod. Phys. D **15**, 1753 (2006).

[2] C. Wetterich, Nucl. Phys. B **302**, 668 (1988); B. Ratra and P.J.E. Peebles, Phys. Rev. D **37**, 3406 (1988); J.A. Frieman, C.T. Hill, A. Stebbins and I. Waga, Phys. Rev. Lett. **75**, 2077 (1995) ; M.S. Turner and M. White, Phys. Rev. D **56**, R4439 (1997); R.R. Caldwell, R. Dave and P.J. Steinhardt, Phys. Rev. Lett. **76**, 1582 (1998); A.R. Liddle and R.J. Scherrer, Phys. Rev. D **59**, 023509 (1999); P.J. Steinhardt, L. Wang, and I. Zlatev, Phys. Rev. D **59**, 123504 (1999).

[3] G.R. Dvali, G. Gabadadze, and M. Porrati, Phys. Lett. B**485**, 208 (2000); C. Deffayet, Phys. Lett. B**502**, 199 (2001); S. Nojiri and S. D. Odintsov, Phys. Rev. D 68, 123512 (2003); S.M. Carroll, V. Duvvuri, M. Trodden, and M.S. Turner, Phys. Rev. D**70**, 043528 (2004); S. Noriji and S.D. Odintsov, Int. J. Geom. Meth. Mod. Phys. **4**, 115 (2007); Y.S. Song, W. Hu, and I. Sawicki, Phys. Rev. D**75**, 044004 (2007); S. Nojiri and S. D. Odintsov, Phys. Rev. D 77, 026007 (2008).

[4] A. Shafieloo, V. Sahni and A. A. Starobinsky, Phys. Rev. D **80**, 101301 (2009) [arXiv:0903.5141 [astro-ph.CO]].

[5] M. Chevallier and D. Polarski, Int. J. Mod. Phys. D **10**, 213 (2001) [arXiv:gr-qc/0009008].

[6] E. V. Linder, Phys. Rev. Lett. **90**, 091301 (2003) [arXiv:astro-ph/0208512].

[7] Z. Li, P. Wu and H. Yu, Phys. Lett. B **695**, 1 (2011) [arXiv:1011.1982 [gr-qc]].

[8] H. Wei, Phys. Lett. B **687**, 286 (2010) [arXiv:0906.0828 [astro-ph.CO]].

[9] V. Mukhanov, *Physical Foundations of Cosmology*, Cambridge (2005).

[10] A.Linde and A. Mezhlumian, Phys. Rev. D **52**, 6789 (1995); A. Linde, D. Linde, A. Mezhlumian, Phys. Lett. B**345**, 203,(1995).

[11] E.V. Linder, Astropart. Phys. **24**, 391 (2005).

[12] D. Polarski and A. Ranquet, Phys. Lett. **B627**, 1 (2005).

[13] Z . Y. Huang, B. Wang and R. K. Su, Int. J. Mod. Phys. A **22**, 1819 (2007).

[14] C. Clarkson, M. Cortes and B. Bassett, JCAP **0708**, 011 (2007).

[15] G. Barenboim, E. Fernandez-Martinez, O. Mena and L. Verde, JCAP **1003**, 008 (2010).

[16] M. Hicken *et al.*, Astrophys. J. **700**, 1097 (2009) [arXiv:0901.4804 [astro-ph.CO]].

[17] R. Amanullah *et al.*, Astrophys. J. **716**, 712 (2010) [arXiv:1004.1711 [astro-ph.CO]].

[18] B. A. Reid *et al.*, Mon. Not. Roy. Astron. Soc. **404**, 60 (2010) [arXiv:0907.1659 [astro-ph.CO]];
B. A. Reid *et al.* [SDSS Collaboration], Mon. Not. Roy. Astron. Soc. **401**, 2148 (2010) [arXiv:0907.1660 [astro-ph.CO]].

[19] G. Hinshaw *et al.* [WMAP Collaboration], Astrophys. J. Suppl. **180**, 225 (2009) [arXiv:0803.0732 [astro-ph]]; E. Komatsu *et al.* [WMAP Collaboration], Astrophys. J. Suppl. **180**, 330 (2009) [arXiv:0803.0547 [astro-ph]].

[20] Y. Wang and P. Mukherjee, Phys. Rev. D **76**, 103533 (2007) [arXiv:astro-ph/0703780].